

Received February 10, 2021, accepted March 22, 2021, date of publication April 20, 2021, date of current version April 28, 2021.

Digital Object Identifier 10.1109/ACCESS.2021.3074127

Bull Sperm Tracking and Machine Learning-Based Motility Classification

PRIYANTO HIDAYATULLAH^{1,2}, TATI L. E. R. MENGKO¹, RINALDI MUNIR¹, AND ANGRAINI BARLIAN³

¹School of Electrical Engineering and Informatics, Institut Teknologi Bandung, Bandung 40132, Indonesia

²Computer Engineering and Informatics Department, Politeknik Negeri Bandung, Bandung 40559, Indonesia

³School of Life Sciences and Technology, Institut Teknologi Bandung, Bandung 40132, Indonesia

Corresponding author: Priyanto Hidayatullah (priyanto@polban.ac.id)

This work was supported by the Lembaga Pengelola Dana Pendidikan (LPDP) RI under Grant PRJ-6897 /LPDP.3/2016.

ABSTRACT Sperm motility measurement using computer assisted sperm analysis (CASA) has been widely accepted as a substitute for manual measurement but still faces several challenges. In the tracking phase, tracking errors caused by detection failure often occur when measuring fresh bull semen. Tracking errors occur for two reasons: (1) the sperm move very fast, which makes them appear blurry, and (2) partial occlusion, which frequently occurs. This study proposes the mean angle of sperm motion and Tracking-Grid to predict the position of the sperm that failed to be detected. The Tracking-Grid has also been found useful in tracking fast-moving sperm. The proposed methods reduce identity switch (ID-switch) and achieve a multi-object tracking overall accuracy (MOTAL) of 73.2. The MOTAL result exhibits 5% less ID-switch and is 15.6 MOTAL points higher than state-of-the-art simple online and real-time tracking with a deep association metric (Deep SORT). The speed achieved is 41.18 frames per second (fps), which is 1.8 times faster than Deep SORT. In sperm motility classification, most researchers use one or several CASA parameters with a static threshold value. Such a method is effective for motile-progressive sperm classification but is less reliable for identifying non-motile-progressive sperm such as vibrating and floating sperm. This study proposes a machine learning-based motility classifier using a support vector machine with three CASA parameters: curvilinear velocity (VCL), straight-line velocity (VSL), and linearity (LIN), which we call the bull sperm progressive motility classifier (BSPMC_{svm3casa}). Experimental results show that BSPMC_{svm3casa}'s mean accuracy is 92.08%, which is 2.51–9.67 points higher than other classification methods.

INDEX TERMS Computer assisted sperm analysis, object tracking, sperm motility classification, sperm tracking.

I. INTRODUCTION

Along with the population growth, the demand for beef for Indonesian citizens is increasing. However, the increase in the amount of beef production is not as fast as the community's increasing meet needs. This deficit was met with imports of a huge value (Rp. 4.27 trillion per year in 2016) and continued to increase from year to year [1]. In Indonesia, artificial insemination technology is the single most applicable reproductive technology for increasing livestock production, especially bull/cow. For the implementation of artificial insemination, high quality cryopreserved bull semen is required. The Lembang Institute for Artificial Insemination

The associate editor coordinating the review of this manuscript and approving it for publication was Davide Patti¹.

(Balai Inseminasi Buatan/BIB, Lembang, Indonesia) is mandated by the government to provide high quality cryopreserved bull semen in sufficient quantity for artificial insemination. To fulfill this role, the Lembang Institute for Artificial Insemination needs to improve its principal activity's performance, which is fresh bull semen quality measurement before cryopreservation. Currently, they perform sperm quality evaluation manually. We believe a similar problem occurs in many developing countries.

There are many sperm quality parameters such as sperm concentration, viability, morphology, pH, and color of the semen [2], [3]. However, many researchers mentioned that motility is the main parameter for sperm quality evaluation. Awad [4], Januskauskas *et al.* [5], and Verstegen *et al.* [6] resume that sperm motility is one of the most important

features associated with semen fertilizing capacity, and for many years has been recognized as essential for sperm fertilization. Zhang *et al.* [7] examined the correlation between bull sperm characteristics with the ability of spermatozoa fertility after artificial insemination (AI) of 9426 females. Their result suggests that sperm linear-motility patterns and swim-up separated sperm motility can provide a valuable assessment of the fertilizing capacity of AI bull. Fitzpatrick *et al.* [8] mentioned, estimating the motility before cryopreservation closely relates to the quality of post-thaw sperm. Simonik *et al.* [9] concluded that sperm motility is one of the indicators most evaluated before and after cryopreservation for bull field fertility. Based on those researches, we focus on sperm motility evaluation of fresh bull semen.”

Manual sperm motility measurement has some significant drawbacks, namely subjectivity, low accuracy, inter-variability, and intra-variability [10], [11]. Computer assisted sperm analysis (CASA) has been widely used to overcome these drawbacks. However, there are still some challenges in using CASA, particularly in measuring sperm motility in fresh bull semen where the speed of sperm is relatively high and partial occlusions frequently occur. In this study, our objective is not to replace the current complete whole CASA system. We aim to improve some critical parts of the CASA system. We first address the limited accuracy and speed of multi-sperm tracking. The second major problem is difficulties in the accuracy of motility classification. These two challenges are detailed in the following sections.

One of the primary hurdles is the limited accuracy and speed of multi-sperm tracking. Several researchers have tried to address this challenge [12]. For example, Sørensen *et al.* [13] used a Particle Filter and a Kalman Filter with a Hungarian algorithm for labeling, which is somewhat similar to the method Jati *et al.* [14] used in their study. In Imani *et al.* [15], the authors employed frame difference background subtraction, and selection of the threshold value was made using a non-linear diffusion filter. In these studies, the samples had low sperm concentrations so that only a few sperm were visible in one field of view, and it was rare for occlusion or passing sperm to occur.

In comparison, Urbano *et al.* [16] used a modified joint probabilistic data association filter with good tracking results. A video sample indicates hundreds of sperm counts in one field of view. However, the speed is relatively low at two frames per second (fps), and the accuracy drops dramatically in the second sample (a 20% disparity). Beya *et al.* [17] extracted several features from the candidate regions; that is, speeded up robust features (SURF), histogram of oriented gradients (HOG), and local binary patterns (LBP). Subsequently, a mean-shift tracking algorithm was applied. In Akbar *et al.* [18], researchers used the Hungarian algorithm to associate sperm between consecutive frames. The inputs of the Hungarian algorithm were sperm coordinates and head direction angle. To speed up performance, Akbar *et al.* [18] used thread programming.

A newer method employed in the field is simple online and real-time tracking with a deep association metric (Deep SORT) [19]. This method has reasonably better tracking speed and accuracy than previous methods. However, the performance is insufficient for robust and real-time tracking of sperm cells in fresh bull semen, which has a high density of sperm cells. In [20], Wojke and Bewley improve Deep SORT by combining it with deep cosine metric learning. There are many variants of metric learning, as mentioned in [21]. Metric learning can also be used for recognition, as in [22].

The second major problem in sperm motility measurement is classification accuracy. Researchers have used different CASA parameters to classify sperm motility. Nafisi *et al.* [23] classified sperm motility using three CASA parameters: linearity (LIN), straight-line velocity (VSL), and sperm head angle variations. The authors used the old 1999 WHO standard [24], in which sperm is categorized into four grades: a (fast motile-progressive), b (slow motile-progressive), c (not progressive), and d (non-motile). However, there was no mention in Nafisi *et al.* study [23] of each parameter's threshold value or the formula combining the three parameters.

In comparison, Urbano *et al.* [16] classified human sperm as motile if the VCL $> 20 \mu\text{m/s}$. This parameter was calculated from two human semen samples, and WHO 2010 standards [25] were followed. Akbar *et al.* [18] classified bull sperm using the LIN parameter. Sperm were classified as “progressive motile” if $\text{LIN} > 0.5$, “motile not progressive” if LIN was between 0.2 and 0.5, and “non-motile” if $\text{LIN} < 0.2$. The standards used were the 2010 WHO standards [25].

In sum, all the studies use a static threshold for classifying sperm motility. The static threshold is effective for motile-progressive sperm classification but less reliable for non-progressive-motile sperm, such as vibrating or floating sperm.

The main contributions of this study are as follows:

1. We present a modified sperm detection model for detecting bull sperm in a video captured in a 500x total magnification setting.
2. We propose using the mean angle of sperm motion and a Tracking-Grid for multi-sperm tracking to predict undetected sperm in the video caused by partial occlusion and the high speed of sperm movement. These methods effectively reduce ID-switch, increasing overall tracking accuracy and speeding up tracking.
3. Unlike previous methods using a static threshold, we propose a machine learning-based sperm motility classification model called bull sperm progressive motility classifier (BSPMC_{svm3casa}), which uses a support vector machine (SVM) with three CASA parameters: VCL, VSL, and LIN.
4. We conduct experiments with real datasets from Balai Inseminasi Buatan Lembang, Indonesia, with specific settings that reduce disputes between observers. Experimental results have shown that our proposed methods

increase precision and speed for tracking as well as accuracy in motility classification.

The remainder of this paper is organized as follows. The experiment's settings, detection model, mean angle of sperm motion, Tracking-Grid, and BSPMC_{svm3casa} are detailed in Section 3. Experimental results are elaborated and discussed in Section 4, and conclusions are offered in Section 5.

II. MATERIALS AND METHODS

A. DATASET

Most datasets used in sperm motility measurement are drawn from experiments using a 100x or 200x magnification setting. Although this magnification level might be sufficient to detect sperm, it has drawbacks such as subjectivity, low accuracy, low repeatability, and high intra- and inter-variability for revealing the ground truth in sperm motility classification [26]–[29]. These limitations derive from problems with the use of manual measurement to reveal ground truth. It is reasonably difficult to manually measure hundreds of small sperm' motility status without any dispute between observers. These challenges reduce the validity of the ground truth. To overcome these limitations, we used a 500x magnification setting so that sperm cells can be observed in more detail. Each sperm is possible to be manually classified, whether it is a progressive or non-progressive.

Twelve fresh sperm samples are diluted with physiological sodium chloride (NaCl) 0.9%. The three sperm concentration settings are 0.1%, 0.5%, and 1.0%. We choose 0.9% physiological NaCl as recommended by Fauzi *et al.* [30]. One of the conditions for a dilution media to meet is similar osmotic pressure with the semen. The 0.9% physiological NaCl has similar osmotic pressure to the semen osmotic pressure with neutral pH, making it suitable for dilution before semen evaluation. We also choose 0.9% physiological NaCl as the sample looks clearer so that the sperm is easier to be detected and tracked. It is undoubtedly crucial to have a clear appearance of sperm to have a high detection accuracy, leading to high tracking and classification accuracy.

When recording sperm movement, an Olympus BX51 phase-contrast microscope with a total magnification of 500x and an eyepiece 2-megapixel universal serial bus (USB) camera are used. This setting allows the observer to properly assess the movement of individual sperm [2]. The video resolution is 640 × 480 pixels, which is recorded at 15 fps. To improve the accuracy of sperm detection, we set the contrast diaphragm microscope to ph.1 to obtain a higher contrast sample.

Three experienced observers from *Balai Inseminasi Buatan Lembang* Indonesia classify each sperm for its motility and we record the data. Motility classification is possible because at a magnification of 500x the sperm is clearly visible, and it is easier to assess motility. For detection, they perform annotation using YOLOmark [31], and for tracking they use the DarkLabel 1.3 application [32].

The training dan validation dataset is taken from the initial 50 frames of the first and the second bull video samples

(100 frames in total), in which the sperm concentration is 0.5% and 1.0%. We randomly choose 80% of the data for the training dataset and the rest for the validation dataset. Although the number of videos for the training dataset is limited, the number of objects annotated is relatively sufficient at 2933. The validation dataset has 739 annotated objects. For the test dataset, we used all three sperm concentration settings to thoroughly test the model in different situations. Two frames are extracted from each of the remaining ten videos, with 525 total objects in the dataset. This composition is suggested by Rosebrock [33] and is useful for testing the models' generalizability against new data [34]. We used the same dataset for all phases, that is, sperm detection, sperm tracking, and motility classification.

B. DETECTION MODEL

This study's sperm tracking method applies detection-based multi-object tracking (tracking by detection). Object tracking researchers commonly use this approach. The coordinates resulting from the detection model become input for the tracking application to determine the position of the sperm in the ensuing frame.

We adopt the DeepSperm model [35], which is developed for bull sperm tracking at a 100x total magnification. According to the YOLOv3 architecture, the sperm recorded using 100x total magnification are considered small-sized objects. On the contrary, objects in the sample of this study are recorded at 500x total magnification, which are considered middle-sized objects. Therefore, we modify DeepSperm architecture to detect middle-size objects by changing its input layer resolution from 640 × 640 into 416 × 416. We also add several convolutional layers and a Resnet block at the end of the architecture. Fig. 1 shows the illustration of the modified architecture. We train the model using the same hyper-parameters, augmentation parameters, and the number of epochs as DeepSperm [35]. The darknet framework [36] is used for the training.

C. SPERM TRACKING METHOD

This study uses a detection-based, multi-object tracking approach, where the multi-object tracking problem can be formulated into (1) to (7) [37]

$$X_k = (x_k^1, x_k^2, \dots, x_k^{M_k}), \quad (1)$$

$$x_{k_s:k_e}^i = \{x_{k_s}^i, \dots, x_{k_e}^i\}, \quad (2)$$

$$X_{1:k} = \{X_1, X_2, \dots, X_k\}, \quad (3)$$

where vector x_k^i is the i^{th} sperm state in the k^{th} frame whereas, $X_k = (x_k^1, x_k^2, \dots, x_k^{M_k})$ is a set of state vectors of all sperm totaling M_k in the k^{th} frame. The notation $x_{k_s:k_e}^i = \{x_{k_s}^i, \dots, x_{k_e}^i\}$ is used to denote the i^{th} set of sperm state vectors where k_s is the initial frame and k_e represents the appearance of sperm in the video's final frame. In (3), $X_{1:k} = \{X_1, X_2, \dots, X_k\}$ represents collections of all sperm

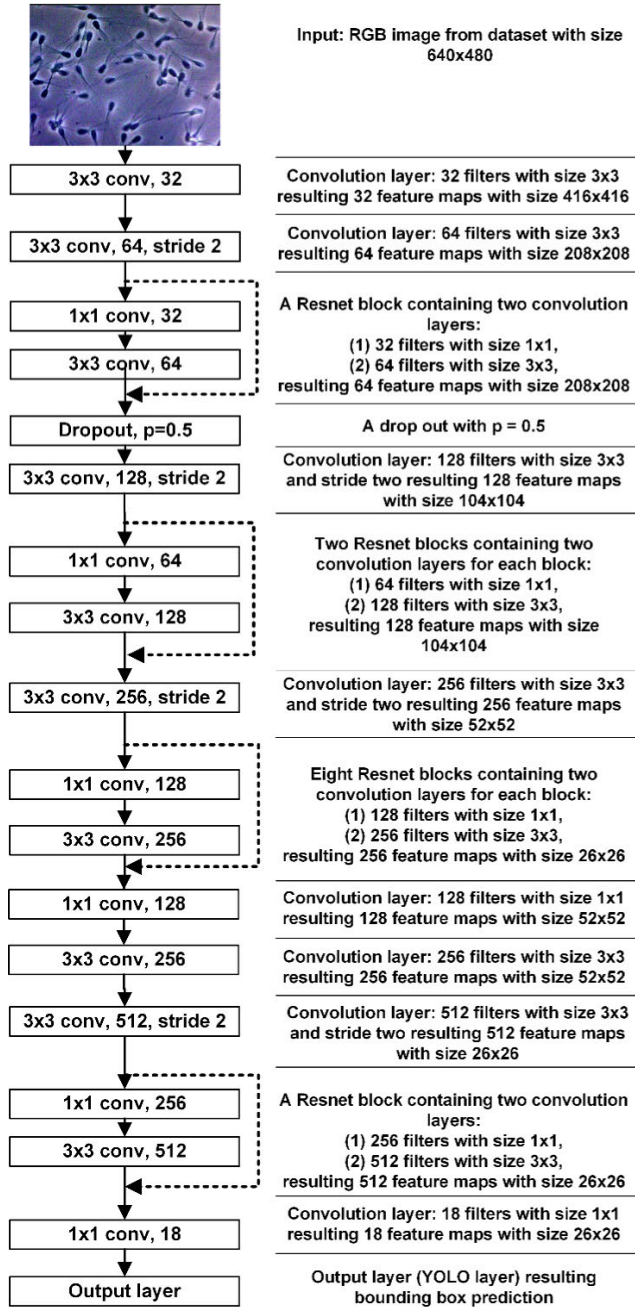


FIGURE 1. Detection model architecture.

objects states ordered from the first frame to the k^{th} frame.

$$Z_k = (z_k^1, z_k^2, \dots, z_k^{M_k}), \quad (4)$$

$$z_{k_s:k_e}^i = \{z_{k_s}^i, \dots, z_{k_e}^i\}, \quad (5)$$

$$Z_{1:k} = \{Z_1, Z_2, \dots, Z_k\}, \quad (6)$$

where z_k^i is the result of the detection of the i^{th} sperm in the k^{th} frame, and $Z_k = (z_k^1, z_k^2, \dots, z_k^{M_k})$ is all sperm detection results totaling M_k in the k^{th} frame. The notation $z_{k_s:k_e}^i = \{z_{k_s}^i, \dots, z_{k_e}^i\}$ is the result of the i^{th} sperm detection where k_s is the initial frame and k_e is the final frame in which sperm

appears in the video. $Z_{1:k} = \{Z_1, Z_2, \dots, Z_k\}$ represents all sets of sperm object detection results sorted from the first frame to the k^{th} frame.

The purpose of detection-based multi-object tracking is to find the optimal vector sequence of objects. These objects can generally be modeled by estimating the maximal a posteriori (MAP) of conditions in a particular frame ($X_{1:k-1}$) with input in the form of total detection results ($Z_{1:k}$), as shown in (7) [37].

$$X_{1:k} = \arg \max_{X_{1:k-1}} P(X_{1:k-1} | Z_{1:k}). \quad (7)$$

The state of the art in multi-object tracking is Deep SORT, which focuses on improving simple online and real-time tracking (SORT) [38] performance in data association by reducing the change in object identity (ID-switch). To achieve this goal, information on the object's appearance is added in addition to using a Kalman filter to predict an object's position based on its movement. The object display information has been trained on the pedestrian dataset. Using this method, Wojke *et al.* [19] claim to reduce ID-switch by 45%.

However, the Kalman filter's use as the central part of the tracker decreases the tracking speed because the Kalman filter requires a reasonably high computation [39]. In this study, a faster method is proposed by not using the Kalman filter. Instead, we propose using the mean angle of sperm motion and the Tracking-Grid to predict the sperm's position in the next frame. The prediction with the mean angle of sperm motion uses standard trigonometric calculations, whereas the Tracking-Grid only considers a small number of detected sperm in the data association phase to reduce computation.

After the sperm detection phase is complete, the tracking model task can accurately associate bull sperm in consecutive frames. Sperm association typically uses sperm coordinates. However, sperm coordinates are often insufficient to produce accurate tracking results in the case of occlusion and sperm that fail to be detected. For that, other methods of increasing tracking accuracy are required. This study proposes to employ the mean angle of sperm motion and the Tracking-Grid to improve multi-sperm tracking accuracy and speed. The overview of the tracking algorithm is displayed in Fig. 2.

1) MEAN ANGLE OF SPERM MOTION

Determining sperm motion direction is crucial because a frequent problem in sperm tracking is occlusion. Moreover, this angle is also vital in tracking when sperm fails to be detected. When such cases occur, the data association based on position alone is insufficient. The mean angle of sperm motion is used to predict the position of the sperm when it fails to be detected. The failure happens due to occlusion or because it appears blurry due to its swift movement.

Akbar *et al.* [18] determine the direction of the sperm from the detection of an elliptical sperm head. However, in this research dataset, the results of the segmentation of sperm from the background are not acceptable. About 40% of the

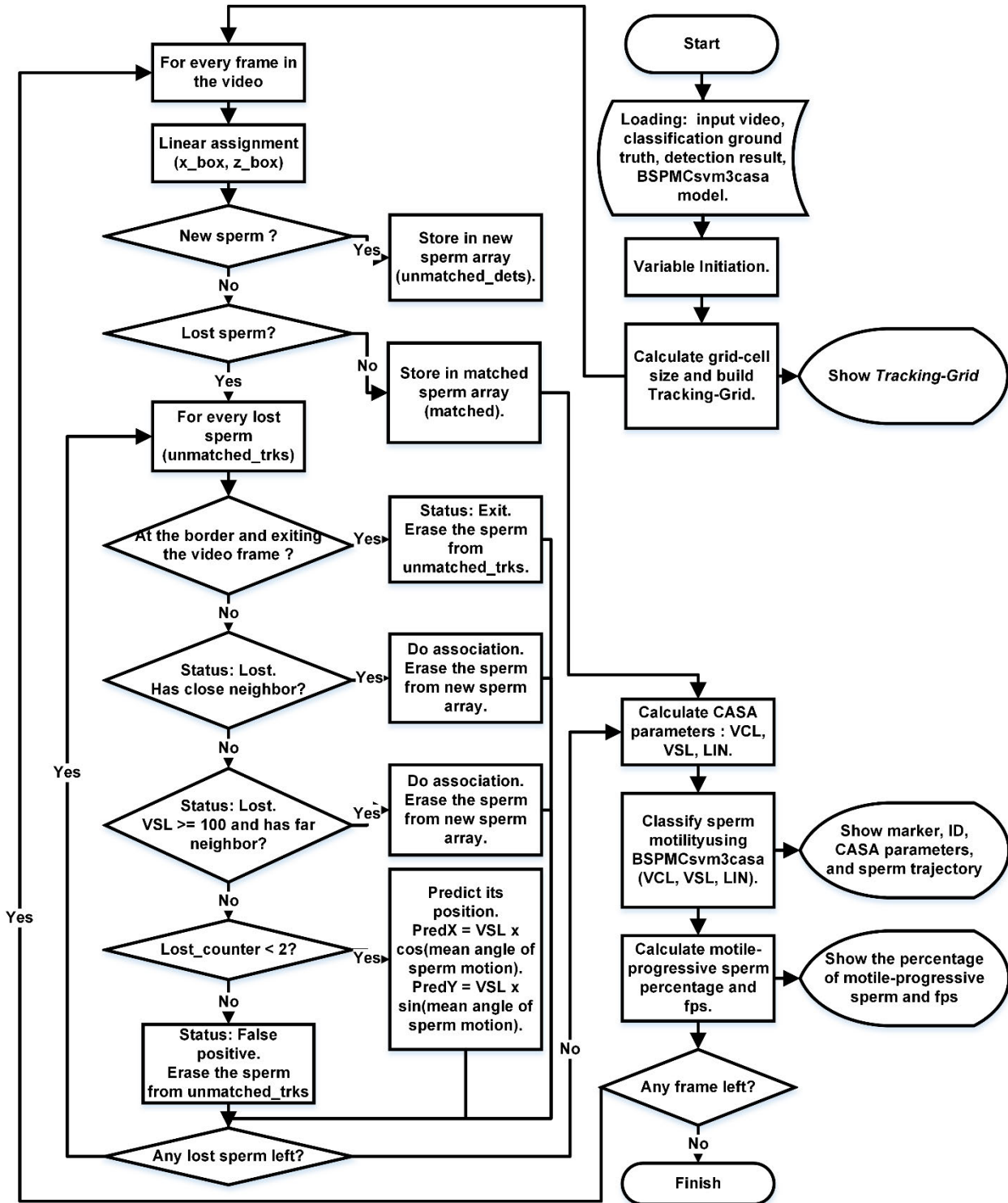


FIGURE 2. The tracking and classification overview.

sperm segmentation results are not perfect ellipses, so the resulting angle is less accurate.

The second drawback of this method is that it is unsuitable for application to sperm with low progressive motility values. For example, floating sperm often does not move in the

direction of the head of the sperm. Instead, it moves because of a push from the surrounding motile sperm or the flow of semen. This study proposes using the mean angle of sperm motion to determine new sperm angles of motion to overcome these drawbacks.

The mean angle of motion of the sperm is calculated based on the displacement of the sperm. The calculation starts from the second frame because the sperm has not moved in the first frame, so it is impossible to know the angle. If a new sperm enters the video's field of view when the video has been running, the angular data will start to be calculated in the second frame after the sperm has entered. The mean angle calculation is then performed two frames later (on the fourth frame after birth) so that the total angles averaged are three angles (3-frame averaged angle). This calculation of the mean angle continues throughout the video. The calculation of the mean angle follows,

$$\bar{\theta}_k^i = \frac{\sum_{k-2}^k \theta_k}{3}, k \in \{4..N\}, \quad (8)$$

where $\bar{\theta}_k^i$, θ_k , and N denote the mean angle of the i^{th} sperm motion in frame k , the angle of sperm motion direction in frame k , and the total number of video frames, respectively.

2) DATA ASSOCIATION

In multi-object tracking, data association is a major challenge. In this study, data association is meant by the association of sperm found in one frame with the sperm in the next frame. The problem formulation is in (1)–(7). Data association is carried out using the Hungarian algorithm. In this study, the Hungarian algorithm's implementation, called the linear assignment, is used from the scikit-learn library [40].

3) SPERM REIDENTIFICATION

Often the detection of sperm fails for some sperm that are difficult to detect in a specific frame. This case occurs, for example, when the sperm is moving rapidly so that at certain times the sperm appears opaque and difficult to detect. Often the sperm is detected again at the next frame. In many tracking methods, the detected sperm is given a new identity so that the tracking path will be interrupted.

For the tracking to remain accurate, and the tracking trajectory to be continuous despite a detection failure, this study proposes sperm reidentification using the mean angle of motion of the sperm and the Tracking-Grid. When some sperm fail to be detected, their positions are predicted using

$$p_k^i = \left(x_{k-1}^{ix} + VSL_{k-1}^i \times \cos \bar{\theta}_{k-1}^i, x_{k-1}^{iy} + VSL_{k-1}^i \times \sin \bar{\theta}_{k-1}^i \right), \quad (9)$$

where p_k^i is the predicted position of the i^{th} sperm in frame k , x_{k-1}^{ix} is the x coordinate of the i^{th} sperm in frame $k - 1$, x_{k-1}^{iy} is the y coordinate of the i^{th} sperm in frame $k - 1$, VSL_{k-1}^i is the straight-line velocity of the i^{th} sperm in frame $k - 1$, and $\bar{\theta}_{k-1}^i$ is the mean angle of motion of the i^{th} sperm in frame $k - 1$.

4) TRACKING-GRID

Occlusion frequently occurs in semen with a high density, as found in this study sample. The occlusion effect

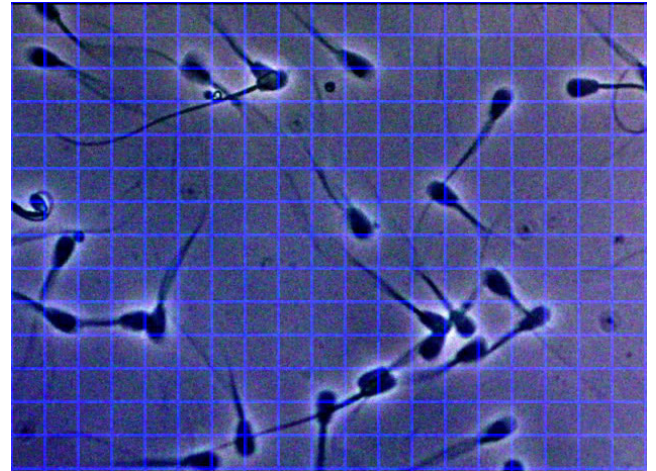


FIGURE 3. Tracking-Grid example.

$G_{j-2,k-2}$	$G_{j-1,k-2}$	$G_{j,k-2}$	$G_{j+1,k-2}$	$G_{j+2,k-2}$
$G_{j-2,k-1}$	$G_{j-1,k-1}$	$G_{j,k-1}$	$G_{j+1,k-1}$	$G_{j+2,k-1}$
$G_{j-2,k}$	$G_{j-1,k}$	$G_{j,k}$	$G_{j+1,k}$	$G_{j+2,k}$
$G_{j-2,k+1}$	$G_{j-1,k+1}$	$G_{j,k+1}$	$G_{j+1,k+1}$	$G_{j+2,k+1}$
$G_{j-2,k+2}$	$G_{j-1,k+2}$	$G_{j,k+2}$	$G_{j+1,k+2}$	$G_{j+2,k+2}$

FIGURE 4. Tracking-Grid illustration. Undetected sperm is in the yellow cell. The close-neighbor area is in green. The far-neighbor area is blue.

on tracking is ID-switch: a tracking error in which there is an exchange of identity numbers between the occluding sperm. In this study, we propose a Tracking-Grid to solve the problem of occlusion. With the Tracking-Grid, the video frame is divided into grid cells where the grid cell's size is half the average sperm size. We choose a half-value because the consensus of determining whether a sperm is counted is when half of the head is visible in the frame. The position in the grid of each sperm is also determined by knowing the neighboring sperm. Fig. 3 shows an example of Tracking-Grid implementation in a video frame.

At the time of occlusion, each sperm is evaluated, and its neighboring sperm are determined. In principle, the sperm move relatively consistently in a particular direction. Therefore, the neighboring sperm is adjacent to it and in the direction of the mean angle of sperm motion. Fig. 4 illustrates how the Tracking-Grid works. For example, the sperm in the grid cell $G_{j,k}$ (colored yellow), have a mean motion angle of 45°

and a center point in this image. Its neighbors are the sperm located in the grid cells $G_{j,k-1}$, $G_{j+1,k-1}$, and $G_{j+1,k}$ (colored green). These sperm are called close neighbors.

There is a particular case where sperm moves very fast. In this condition, the sperm in the next frame sometimes does not overlap with the sperm in the current frame. Often the sperm is considered lost (undetected), and the sperm in the next frame is given a new identity. The Tracking-Grid addresses this problem by identifying a fast-moving sperm from its velocity. If the $VSL \geq 62.38 \mu\text{m/s}$, then the sperm is considered as a fast-moving sperm. Far neighbors are rapid sperm located farther apart. In the previous example, the far neighbors are grid cells $G_{j,k-2}$, $G_{j+1,k-2}$, $G_{j+2,k-2}$, $G_{j+2,k-1}$, and $G_{j+2,k}$ (colored blue).

The benefit of the Tracking-Grid and the mean angle, apart from predicting the position of the sperm in the next frame more accurately, is computational efficiency. This benefit derives from not having to examine all sperm surrounding sperm in the grid cell $G_{j,k}$. It is sufficient to only check the close neighbors or far neighbors (for fast-moving sperm).

5) SPERM TRACKING EVALUATION

We use the test dataset from BIB Lembang for evaluation. Evaluation is performed on the proposed method and the state-of-the-art method to see whether the proposed method has significant improvements. We use the standard multi-object tracking metric 16 (MOT16) [41] as a measuring tool to compare the accuracy performance and fps for speed.

D. SPERM CLASIFICATION MODEL

The final part of this research is to develop a method of sperm motility classification.

1) CALCULATION OF CASA PARAMETERS FROM SPERM TRACKING RESULTS

The next process after sperm tracking is to calculate the percentage of progressive-motile sperm. Veterinarians need this information at the artificial insemination center to decide whether the tested semen sample is qualified for preservation. The process begins with calculating the CASA parameters based on the results of sperm tracking. The model classifies the sperm motility from these CASA parameters. In the WHO laboratory manual, sperm are classified into three categories, namely progressively motile, non-progressively motile, and immotile. In BIB Lembang, the veterinarians use two categories, motile-progressive and non-motile-progressive. Non-progressively motile and immotile sperm based on the WHO standard are categorized as non-motile-progressive sperm. Included in this category are static, floating, and vibrating sperm.

Several researchers [16], [18], [23], [42] use one or more of CASA parameters in classifying sperm motility. In this study, we calculate three CASA parameters, which are VCL, VSL, and LIN. These three parameters are calculated using the equations in (10)–(12) [25], [43], [44]. For determining sperm velocity (VCL and VSL) in $\mu\text{m/s}$ units, we use an

improved Neubauer counting chamber [45] to determine the pixels to μm scale.

$$VCL_i = \frac{\sum_{j=1}^M \sqrt{(x_{j+1} - x_j)^2 + (y_{j+1} - y_j)^2}}{(M - 1) \Delta t}, \quad (10)$$

$$VSL_i = \frac{\sqrt{(x_M - x_1)^2 + (y_M - y_1)^2}}{(M - 1) \Delta t}, \quad (11)$$

$$LIN_i = \frac{VSL_i}{VCL_i}, \quad (12)$$

where VCL_i is the average velocity of i^{th} sperm on the actual trajectory for Δt duration, and M is the number of points in the trajectory. VSL_i is the average velocity of i^{th} sperm along a straight line connecting the initial position to the end position of the sperm M in Δt duration. LIN_i is the linearity of the i^{th} sperm motion, which is defined as the ratio between VSL_i and VCL_i . The x and y are the coordinates of the sperm.

2) CLASSIFICATION OF SPERM MOTILITY BASED ON BSPMC_{svm3casa}

Based on the WHO laboratory manual [25], sperm motility analysis using CASA can be done with a minimum of 1 s video duration. However, in this study, the videos used are 1–5 s in duration to test the methods' reliability. A classification model is built using an SVM with a linear kernel. We use the same training and test dataset as for the detection model, naming the classification model as BSPMC_{svm3casa}.

The proposed classification model has three input CASA parameters: VCL, VSL, and LIN. The output is the classification result of whether the sperm is included in the progressive-motile sperm class. The model is trained to find the w_i weight parameter that provides the most appropriate classification according to the classification ground truth. Equation (13) is the target function representation

$$y = b + (w_1 \times VCL) + (w_2 \times VSL) + (w_3 \times LIN). \quad (13)$$

From the learning results, the values of w_i and b are obtained so that we have the estimation function

$$y = -4.080 + (0,060 \times VCL) + (0,008 \times VSL) + (2,136 \times LIN), \quad (14)$$

$$\hat{y} = \begin{cases} -1 \text{ (non-motileprogressive)}, & y < 0, \\ +1 \text{ (motileprogressive)}, & y > 0, \end{cases}$$

where \hat{y} is output in the form of sperm classification, w_i is the i^{th} weight from training results, and b is bias.

3) EVALUATION OF SPERM MOTILITY CLASSIFICATION RESULTS

After the method has been successfully developed, the final step is testing to assess its performance. The performance is measured from the conformity with the results of manual classification conducted by veterinarians from BIB Lembang. In the newest available WHO laboratory manual (2010 5th

edition) [25], sperm should be classified into three classifications: progressively motile, non-progressively motile, and immotile. For bull sperm motility assessment, especially in practice, what the Artificial Insemination Centers need is the percentage of progressively motile sperm. Therefore, the classification of WHO can be used but with modification. For bull sperm, classifying the sperm motility into two classes is sufficient: (a) progressively motile and (b) a class consists of non-progressively motile and immotile [2]. The value of the percentage of motility is calculated based on the ratio of sperm that moves actively forward (progressive motile) to the total sperm [2].

E. OVERALL EVALUATION

A CASA system consists of three main processes: sperm detection, tracking, and classification. In this study, we proposed methods to improve the performance of those processes. To evaluate the effectiveness of our proposed methods to the current CASA system, we compare the performance of a bull sperm CASA system by Akbar *et al.* [18] before and after improved using our proposed methods.

F. EXPERIMENTAL ENVIRONMENT

Model training and testing employed an Intel Core i7 8700 @3.2 GHz workstation with 16 GB RAM. The operating system was an Ubuntu 16.04 LTS. A single NVIDIA GeForce RTX 2070 8 GB GPU RAM was used with 7.5 compute capability points, which is considered sufficient for training and testing in this case.

III. RESULTS AND DISCUSSION

A. SPERM DETECTION RESULTS

With the dataset and experimental setting of this study, the detection model converged at 2400 epochs out of 4000 training epochs. With 1.515 s of training time needed for an epoch, we achieve convergence in 60.6 minutes. The achieved accuracy is also considerably high, with a 98.4 mean average precision (mAP) validation accuracy and 95.09 mAP test accuracy.

B. SPERM TRACKING RESULTS

Tracking accuracy affects classification accuracy. Tracking accuracy is the most critical criterion in tracking because the artificial insemination center demands an accurate sperm motility classification. The video sample tests yielded a total of 414 sperm trajectories. Of these trajectories, 233 can be tracked well (“mostly tracked” (MT)). Whereas Deep SORT mostly tracks 121 trajectories. The multi-object tracking accuracy (MOTA) of the proposed method is 70.9, with the multi-object tracking precision (MOTP) reaching 73.0 and multi-object tracking overall accuracy (MOTAL) is 73.2. On the other hand, Deep SORT achieves an accuracy of 55.2 and a precision of 72.7 and total accuracy of 57.6.

Some fast-moving sperm failed to be detected. The assumption that sperm always exists in the video frame except

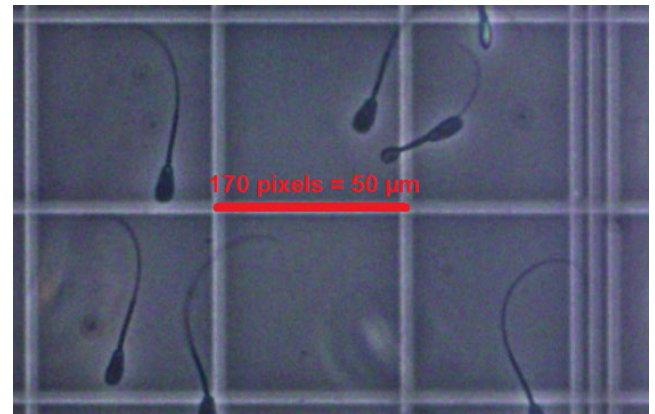


FIGURE 5. Finding scale from pixel to μm .

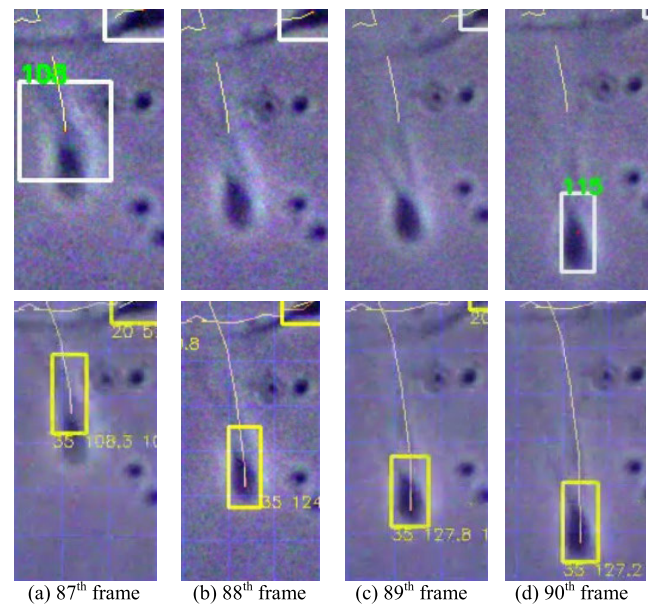


FIGURE 6. Illustration of ID-switch on Deep SORT when the sperm is moving very fast. Deep SORT (top row); Tracking-Grid (bottom row).

if it exits the frame is valid for this study case. Based on this assumption, a prediction of the position of the sperm is carried out. This prediction follows (9). Beforehand, we need to convert between pixel distance in a video frame into μm to calculate CASA parameters. Based on the calibration using the improved Neubauer chamber in our experiment setting, we obtain that 1 pixel is $0.29412 \mu\text{m}$. Fig. 5 illustrates the process of finding the scale.

The proposed method managed detection failure cases to reduce the switch ID from 147 cases to 133 cases (a 10% reduction). Fig. 6 shows an ID-switch illustration due to the fast-moving sperm ($\text{VSL} \geq 62.5 \mu\text{m/s}$). The first row in Fig. 6 is sperm tracked using Deep SORT. On the 88th and 89th frames, some detection failures occurred. Deep SORT gives a new identity to the sperm that failed to be detected from 108 to 115.

On the other hand, in the proposed method, at frame 88 and 89, the position is predicted using (9). At the 90th frame, the sperm can be redetected. Tracking-Grid (Fig. 4) is used

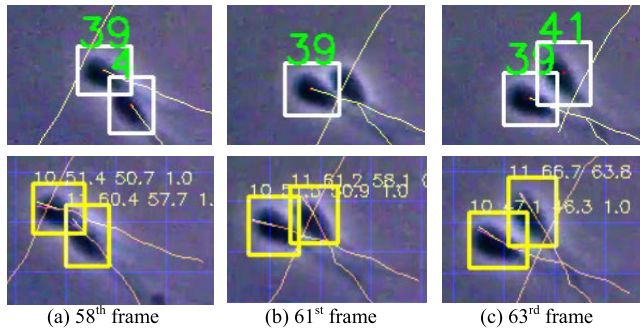


FIGURE 7. Illustration of ID-switch on Deep SORT during occlusion. Deep SORT (top row), Tracking-Grid (bottom row).

to check whether the sperm is neighbors. Once confirmed, the new detection result is given the same identification number as the sperm on the 88th frame. The result is that the sperm can be appropriately tracked, and the identity of the sperm can be maintained.

In addition to rapid sperm movement, occlusion is also a cause of identity switch. Fig. 7 illustrates occlusion. In the first row of Fig. 7, sperm number 4 fails to be detected when it crosses sperm number 39 (at frame 61). At the 63rd frame, sperm number 4 is given a new identity (i.e., 41). However, in the proposed method (Fig. 7 second row), sperm number 11, which fails to be detected at frame 61, its identity number can be retained. It is possible because when sperm number 11 fails to be detected, its position in that frame is predicted according to (9) and given the same identity number (i.e., 11). Subsequently, at frame 63, when the sperm can be redetected, it is checked whether the detection result is a neighbor of sperm number 11 based on Fig. 4. After it is known that the detection result is the neighbor, it is given the same identity number (i.e., 11).

The tracking implementation must be able to run at high speed to be used in practice. The proposed method reaches a speed of 41.18 fps. This speed is 1.8x faster than the Deep SORT speed of 23.44 fps. The Kalman filter computation has a significant share of the limited speed of Deep SORT. Whereas, in the proposed method, prediction is carried out employing data association using the mean angle of sperm motion and Tracking-Grid, for which the computation is not as heavy as the Kalman filter.

Wojke and Bewley [20] improve the performance by combining Deep SORT with deep cosine metric learning. We do the training of their convolutional neural network for 100,000 iterations as suggested in the paper [20] and choose the last checkpoints as it gives the best validation accuracy. We fine-tune the minimum detection threshold to have the best possible detection accuracy and found that 0.01 gives the best result.

The result is accuracy and speed are both increased. Though the ID-switch is increased slightly, the overall accuracy (MOTAL) is increased by 0.7 points. The significant improvement is the speed, which is 1.3x faster than Deep SORT.

TABLE 1. Tracking results comparison.

Metric	Deep SORT	Deep SORT + Deep Cosine Metric Learning	Tracking-Grid*
MOTAL	57.6	58.3	73.2
MOTA	55.2	55.9	70.9
MOTP	72.7	72.4	73.0
MT	121	137	233
PT	176	174	109
ML	75	70	36
IDsw	207	211	197
FPS	23.44	30.67	41.18

* the proposed method

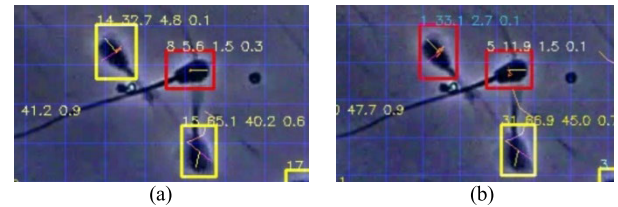


FIGURE 8. Comparison of classification with VCL (a) and BSPMC_{svm3casa} (b).

We present the tracking results in tabular form to make it easier to compare findings. This table contains Deep SORT and Tracking-Grid results with standard multi-object tracking metrics MOT-16 [41]. Table 1 displays the comparison with the values in bold, showing the best values after comparison.

C. SPERM CLASSIFICATION RESULTS

Motility classification performance is measured by calculating the difference between the classification result from the system (compared methods) and the classification ground truth from the manual measurement. With the settings mentioned in the Dataset section, there is no dispute between observers in making ground truth classifications. In this study, a comparison of the effectiveness of several proposed CASA parameters for classifying bull sperm motility is conducted. We choose two recent studies for comparison, Urbano *et al.* [16] and Akbar *et al.* [18]. In both studies, manual static threshold values are used. To maintain fairness in comparison, all classification methods are fed with the same input which is come from detection and tracking results using our proposed methods.

The BSPMC_{svm3casa} is a classifier model that uses several CASA parameters: VCL, VSL, and LIN. This model is not only able to better classify progressive-motile sperm but also non-progressive-motile sperm. In the third test sample video, there is a vibrating sperm. This sperm has a high VCL value. However, based on the WHO standard, it is not classified as a motile-progressive sperm. One of the reasons is because the position of the sperm is generally unchanging. Therefore, even though we have searched for an optimal threshold value, the use of VCL alone in determining sperm motility is insufficient.

In Fig. 8, four pieces of information are displayed for each sperm: the identity number (ID), VCL, VSL, and LIN. The yellow indicates that the sperm is classified as

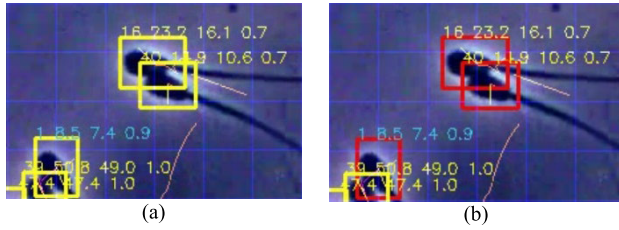


FIGURE 9. Comparison of classification with LIN (a) and BSPMC_{svm3casa} (b).

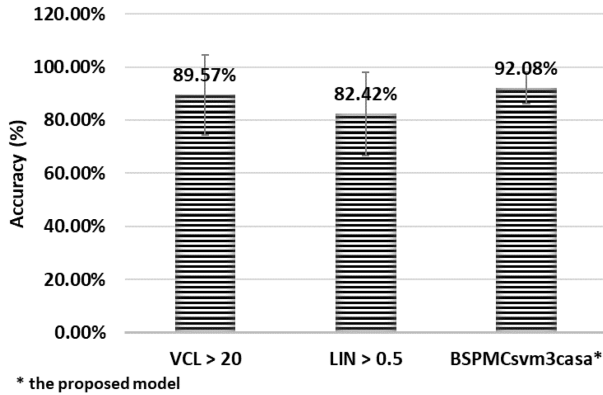


FIGURE 10. Comparison of the mean accuracy of the classification results.

motile-progressive sperm, whereas red indicates that the sperm is non-motile-progressive. This figure provides an illustration of the failure of sperm motility classification in vibrating non-motile-progressive sperm. Sperm with an ID number of 8 (ID number 1 in Fig. 8 (b)) is an example of this type of sperm, whose characteristics are that the VCL value is relatively high but the VSL (and the LIN) is small. If only VCL is used in the classification, the sperm is classified as motile-progressive sperm (yellow bounding box) because the VCL is above the threshold (20 $\mu\text{m/s}$). However, when using BSPMC_{svm3casa}, this sperm can be correctly classified as non-motile-progressive sperm (Fig. 8(b)).

In one of the samples, some dead sperm are continually moving toward the lower left. These sperm are called floating sperm because they move in constant motion with high VCL and VSL values but an inactive manner. In addition to high VCL and VSL values, these sperm have a higher LIN value than others because they move relatively linear and do not vibrate like normal motile sperm. Therefore, using only LIN failed to classify this type of sperm irrespective of the manner of finding the best threshold value.

Fig. 9 illustrates the failure of sperm motility classification in floating non-motile-progressive sperm. Sperm numbers 1, 16, and 40 are floating sperm with relatively high linearity values (0.7 and 0.9). If we use only LIN in the classification, these sperm are classified as motile-progressive sperm because $LIN > 0.5$. However, when using BSPMC_{svm3casa}, these three sperm can be correctly classified as non-motile-progressive sperm (red bounding boxes).

Fig. 10 shows the classification results' mean accuracy using various CASA parameters, including their standard

deviation. From the experiment's findings, we can observe that the mean accuracy of the classification results using BSPMC_{svm3casa} outperforms the accuracy of results from all other methods. Besides failing in the condition in Fig. 8 and Fig. 9, the other methods also failed to correctly classify sperm that moves in a small circle.

In Fig. 10, from left to right, the standard deviations for each method are 15.1, 15.8, and 5.9, respectively. The small standard deviation can be achieved as the proposed model is a machine learning-based model and considers three CASA parameters at a time. Therefore, it is more adaptive to different kind of sperm movement and gives relatively good accuracy to all test samples. On the other hand, the other methods consider one CASA parameter only which give very good result in some cases and drop the accuracy significantly in some other cases. The experiment's results also show that using VCL provides better classification accuracy than using LIN.

D. OVERALL RESULTS

In the previous results section, we compare the performance of our proposed methods with the corresponding previous works separately. For evaluating the effectiveness of our proposed method in the overall CASA system process, we compare Akbar *et al.* [18] CASA system's performance without and with our proposed method. Beforehand, we do some modification to Akbar *et al.* CASA system as it is originally designed for measuring bull sperm motility using 100x total magnification. The purpose is to have the best possible Akbar *et al.* CASA system's performance to this study's dataset. After many experiments, the best performance is achieved when we set MIN_HEAD_SIZE = 16, MAX_HEAD_SIZE = 48, mean filter kernel size = 12, and remove morphology operations in its detection process. We achieve 67.22% motility classification accuracy with the speed of 3.04 fps whereas, after improvement using our proposed method, we achieve 92.08% accuracy (24.86 points more accurate) and 11.18 fps (3.67 times faster).

IV. CONCLUSION

This study presents a modified model for detecting sperm from fresh bull semen recorded using 500x magnification and achieving encouraging accuracy. For tracking, this research proposes using the mean angle of sperm motion and the Tracking-Grid to reduce the ID-switch and increase the tracking accuracy and speed, which surpasses state-of-the-art performance. In the sperm classification process, in contrast to previous methods that use a static threshold, we propose BSPMC_{svm3casa}, a machine learning-based bull sperm motility classifier model using SVM with three CASA parameters: VCL, VSL, and LIN. The classification results also show that the proposed method outperforms previous methods. A further use could be implementing the proposed model and method in a portable single-board circuit mobile device to inspect post thawed cryopreserved bull semen in farms. This model can also be used for other cases, such as examining

bull sperm in 3-dimensions or with different magnifications, examining human sperm, or examining other medical objects.

ACKNOWLEDGMENT

The authors thank Suprpto, Rudi Harsono, Iman Sukirman, Fahmy Avicenna, Dr. Asep Kurnia, and Tri Harsi for recording and annotating the samples. The authors also thank Reza Kahar Aziz, Ph.D., for meaningful feedback.

REFERENCES

- [1] *Outlook Daging Sapi: Komoditas Pertanian Subsektor Peternakan*, Sekretaris Jenderal-Kementerian Pertanian, Pusat Data dan Sistem Informasi Pertanian, South Jakarta, Indonesia, 2016.
- [2] R. I. Arifiantini, *Teknik Koleksi dan Evaluasi Semen pada Hewan*, 1st ed. Bogor, Indonesia: IPB Press, 2012.
- [3] B. Hafez and E. S. E. Hafez, Eds., *Reproduction in Farm Animals*, 7th ed. Philadelphia, PA, USA: Lippincott Williams & Wilkins, 2000.
- [4] M. M. Awad, "Effect of some permeating cryoprotectants on CASA motility results in cryopreserved bull spermatozoa," *Animal Reproduction Sci.*, vol. 123, nos. 3–4, pp. 157–162, Feb. 2011.
- [5] A. Januskauskas, J. Gil, L. Söderquist, M. G. M. Hrd, M. C. Hrd, A. Johannisson, and H. Rodriguez-Martinez, "Effect of cooling rates on post-thaw sperm motility, membrane integrity, capacitation status and fertility of dairy bull semen used for artificial insemination in Sweden," *Theriogenology*, vol. 52, no. 4, pp. 641–658, Sep. 1999, doi: 10.1016/S0093-691X(99)00159-4.
- [6] J. Versteegen, M. Iguer-Ouada, and K. Onclin, "Computer assisted semen analyzers in andrology research and veterinary practice," *Theriogenology*, vol. 57, no. 1, pp. 149–179, Jan. 2002.
- [7] B. R. Zhang, B. Larsson, N. Lundeheim, and Rodriguez-Martinez, "Sperm characteristics and zona pellucida binding in relation to field fertility of frozen-thawed semen from dairy AI bulls: Sperm characteristics and ZP-binding relative to non-return rate," *Int. J. Androl.*, vol. 21, no. 4, pp. 207–216, Jul. 1998, doi: 10.1046/j.1365-2605.1998.00114.x.
- [8] L. A. Fitzpatrick, G. Fordyce, M. R. McGowan, J. D. Bertram, V. J. Doogan, J. De Faveri, R. G. Miller, and R. G. Holroyd, "Bull selection and use in northern Australia," *Animal Reproduction Sci.*, vol. 71, nos. 1–2, pp. 39–49, May 2002, doi: 10.1016/S0378-4320(02)00024-6.
- [9] O. Simonik, J. Sichter, A. Krejcarikova, R. Rajmon, L. Stadnik, J. Beran, M. Dolezalova, and Z. Biniova, "Computer assisted sperm analysis—The relationship to bull field fertility, possible errors and their impact on outputs: A review," *Indian J. Animal Sci.*, vol. 85, no. 1, pp. 3–11, 2015.
- [10] J. Auger, "Intra- and inter-individual variability in human sperm concentration, motility and vitality assessment during a workshop involving ten laboratories," *Hum. Reproduction*, vol. 15, no. 11, pp. 2360–2368, Nov. 2000, doi: 10.1093/humrep/15.11.2360.
- [11] M. K. Hoogewijs, S. P. De Vliegher, J. L. Govaere, C. De Schauwer, A. De Kruif, and A. Van Soom, "Influence of counting chamber type on CASA outcomes of equine semen analysis: Counting chamber type influences equine semen CASA outcomes," *Equine Vet. J.*, vol. 44, no. 5, pp. 542–549, Sep. 2012, doi: 10.1111/j.2042-3306.2011.00523.x.
- [12] P. Hidayatullah, T. L. E. R. Mengko, and R. Munir, "A survey on multisperm tracking for sperm motility measurement," *Int. J. Mach. Learn. Comput.*, vol. 7, no. 5, pp. 144–151, Oct. 2017, doi: 10.18178/ijmlc.2017.7.5.637.
- [13] L. Sørensen, J. Østergaard, P. Johansen, and M. de Bruijine, "Multi-object tracking of human spermatozoa," *Proc. SPIE*, vol. 6914, Mar. 2008, Art. no. 69142C, doi: 10.1117/12.771135.
- [14] G. Jati, A. A. S. Gunawan, S. W. Lestari, W. Jatmiko, and M. H. Hilman, "Multi-sperm tracking using hungarian Kalman filter on low frame rate video," in *Proc. Int. Conf. Adv. Comput. Sci. Inf. Syst. (ICACSIS)*, Malang, Indonesia, Oct. 2016, pp. 530–535, doi: 10.1109/ICACSIS.2016.7872796.
- [15] N. Teyfour, Y. Imani, M. Ahmadzadeh, and M. Golabbakhsh, "A new method for multiple sperm cells tracking," *J. Med. Signals Sensors*, vol. 4, no. 1, p. 35, 2014, doi: 10.4103/2228-7477.128436.
- [16] L. F. Urbano, P. Masson, M. VerMilyea, and M. Kam, "Automatic tracking and motility analysis of human sperm in time-lapse images," *IEEE Trans. Med. Imag.*, vol. 36, no. 3, pp. 792–801, Mar. 2017, doi: 10.1109/TMI.2016.2630720.
- [17] O. Beya, M. Hittawe, D. Sidibe, and F. Meriaudeau, "Automatic detection and tracking of animal sperm cells in microscopy images," in *Proc. 11th Int. Conf. Signal-Image Technol. Internet-Based Syst. (SITIS)*, Bangkok, Thailand, Nov. 2015, pp. 155–159, doi: 10.1109/SITIS.2015.111.
- [18] A. Akbar, E. Sukmawati, D. Utami, M. Nuriyadi, I. Awaludin, and P. Hidayatullah, "Bull sperm motility measurement improvement using sperm head direction angle," *TELKOMNIKA, Telecommun. Comput. Electron. Control*, vol. 16, no. 4, p. 1642, Aug. 2018, doi: 10.12928/telkomnika.v16i4.8685.
- [19] N. Wojke, A. Bewley, and D. Paulus, "Simple online and realtime tracking with a deep association metric," Mar. 2017, *arXiv:1703.07402*. Accessed: Jun. 5, 2020. [Online]. Available: <http://arxiv.org/abs/1703.07402>
- [20] N. Wojke and A. Bewley, "Deep cosine metric learning for person re-identification," in *Proc. IEEE Winter Conf. Appl. Comput. Vis. (WACV)*, Mar. 2018, pp. 748–756.
- [21] M. Kaya and H. S. Bilge, "Deep metric learning: A survey," *Symmetry*, vol. 11, no. 9, p. 1066, 2019.
- [22] X. Zhou, Z. Wei, M. Xu, S. Qu, and G. Guo, "Facial depression recognition by deep joint label distribution and metric learning," *IEEE Trans. Affect. Comput.*, early access, Sep. 8, 2020, doi: 10.1109/TAFFC.2020.3022732.
- [23] V. R. Nafisi, M. H. Moradi, and M. H. Nasr-Esfahani, "A template matching algorithm for sperm tracking and classification," *Physiol. Meas.*, vol. 26, no. 5, pp. 639–651, Oct. 2005, doi: 10.1088/0967-3334/26/5/006.
- [24] *WHO Laboratory Manual for the Examination of Human Semen and Sperm-Cervical Mucus Interaction*, 4th ed., World Health Org., Cambridge Univ. Press, Cambridge, U.K., 1999.
- [25] *WHO Laboratory Manual for the Examination and Processing of Human Semen*, 5th ed., World Health Org., Geneva, Switzerland, 2010.
- [26] G. M. Centola, "Comparison of manual microscopic and computer-assisted methods for analysis of sperm count and motility," *Arch. Androl.*, vol. 36, no. 1, pp. 1–7, Jan. 1996, doi: 10.3109/01485019608987878.
- [27] M. L. W. J. Broekhuijse, E. Šoštarić, H. Feitsma, and B. M. Gadella, "Additional value of computer assisted semen analysis (CASA) compared to conventional motility assessments in pig artificial insemination," *Theriogenology*, vol. 76, no. 8, pp. 1473.e1–1486.e1, Nov. 2011, doi: 10.1016/j.theriogenology.2011.05.040.
- [28] K. Coetzee, T. F. Kruger, and C. J. Lombard, "Repeatability and variance analysis on multiple computer-assisted (IVOS*) sperm morphology readings," *Andrologia*, vol. 31, no. 3, pp. 163–168, May 1999, doi: 10.1046/j.1439-0272.1999.00257.x.
- [29] Á. Nagy, T. Polichronopoulos, A. Gáspárdy, L. Solti, and S. Cseh, "Correlation between bull fertility and sperm cell velocity parameters generated by computer-assisted semen analysis," *Acta Veterinaria Hungarica*, vol. 63, no. 3, pp. 370–381, Sep. 2015, doi: 10.1556/004.2015.035.
- [30] M. Fauzi, W. S. Rachmawati, and E. Pramono, "The effect of physiological NaCl dilution levels and storage duration to sperm motility and abnormality in Muscovy duck," *Animal Prod.*, vol. 3, no. 2, pp. 1–12, May 2001.
- [31] A. Bochkovskiy. (2019). *Yolo_Mark: Windows & Linux GUI for Marking Bounded Boxes of Objects in Images for Training Yolo V3 and V2*. Accessed: Aug. 24, 2019. [Online]. Available: https://github.com/AlexeyAB/Yolo_mark
- [32] Lee. (Jul. 18, 2017). *DarkLabel (Video/Image Labeling and Annotation Tool)*. Accessed: Jun. 30, 2020. [Online]. Available: <https://darkpgmr.tistory.com/16>
- [33] A. Rosebrock, *Deep Learning for Computer Vision With Python: Starter Bundle*, 1st ed. Philadelphia, PA, USA: PyImageSearch, 2017.
- [34] A. Zheng, *Evaluating Machine Learning Models: A Beginner's Guide to Key Concepts and Pitfalls*, 1st ed. Sebastopol, CA, USA: O'Reilly Media, 2015.
- [35] P. Hidayatullah, X. Wang, T. Yamasaki, T. L. E. R. Mengko, R. Munir, A. Barlian, E. Sukmawati, and S. Suprpto, "DeepSperm: A robust and real-time bull sperm-cell detection in densely populated semen videos," Mar. 2020, *arXiv:2003.01395*. Accessed: Aug. 31, 2020. [Online]. Available: <http://arxiv.org/abs/2003.01395>
- [36] A. Bochkovskiy. (Aug. 24, 2019). *Windows and Linux Version of Darknet Yolo V3 & V2 Neural Networks for Object Detection (Tensor Cores are Used)*: AlexeyAB/Darknet. Accessed: Aug. 24, 2019. [Online]. Available: <https://github.com/AlexeyAB/darknet>
- [37] W. Luo, J. Xing, A. Milan, X. Zhang, W. Liu, X. Zhao, and T.-K. Kim, "Multiple object tracking: A literature review," May 2014, *arXiv:1409.7618*. Accessed: Jun. 10, 2020. [Online]. Available: <http://arxiv.org/abs/1409.7618>

- [38] A. Bewley, Z. Ge, L. Ott, F. Ramos, and B. Upcroft, "Simple online and realtime tracking," in *Proc. IEEE Int. Conf. Image Process. (ICIP)*, Phoenix, AZ, USA, Sep. 2016, pp. 3464–3468, doi: [10.1109/ICIP.2016.7533003](https://doi.org/10.1109/ICIP.2016.7533003).
- [39] V. Vaidehi and C. N. Krishnan, "Computational complexity of the Kalman tracking algorithm," *IETE J. Res.*, vol. 44, no. 3, pp. 125–134, May 1998, doi: [10.1080/03772063.1998.11416038](https://doi.org/10.1080/03772063.1998.11416038).
- [40] F. Pedregosa, G. Varoquaux, A. Gramfort, V. Michel, B. Thirion, O. Grisel, M. Blondel, P. Prettenhofer, R. Weiss, V. Dubourg, J. Vanderplas, A. Passos, and D. Cournapeau, "Scikit-learn: Machine learning in python," *J. Mach. Learn. Res.*, vol. 12, pp. 2825–2830, Nov. 2011.
- [41] A. Milan, L. Leal-Taixe, I. Reid, S. Roth, and K. Schindler, "MOT16: A benchmark for multi-object tracking," May 2016, *arXiv:1603.00831*. Accessed: Jun. 10, 2020. [Online]. Available: <http://arxiv.org/abs/1603.00831>
- [42] M. Kraemer, C. Fillion, B. Martin-Pont, and J. Auger, "Factors influencing human sperm kinematic measurements by the Celltrak computer-assisted sperm analysis system," *Hum. Reproduction*, vol. 13, no. 3, pp. 611–619, Mar. 1998, doi: [10.1093/humrep/13.3.611](https://doi.org/10.1093/humrep/13.3.611).
- [43] P. Hidayatullah, I. Awaludin, R. D. Kusumo, and M. Nuriyati, "Automatic sperm motility measurement," in *Proc. Int. Conf. Inf. Technol. Syst. Innov. (ICITSI)*, Bandung, Indonesia, Nov. 2015, pp. 1–5, doi: [10.1109/ICITSI.2015.7437674](https://doi.org/10.1109/ICITSI.2015.7437674).
- [44] Ł. Witkowski, "An automatic system for calculating basic semen parameters," *TASK Quart., Sci. Bull. Acad. Comput. Centre Gdansk*, vol. 8, no. 2, p. 6, 2004.
- [45] E. Bailey, N. Fenning, S. Chamberlain, L. Devlin, J. Hopkisson, and M. Tomlinson, "Validation of sperm counting methods using limits of agreement," *J. Androl.*, vol. 28, no. 3, pp. 364–373, Dec. 2006, doi: [10.2164/jandrol.106.002188](https://doi.org/10.2164/jandrol.106.002188).



PRIYANTO HIDAYATULLAH received the bachelor's degree from the Department of Informatics, Institut Teknologi Bandung, Indonesia, in 2004, and the Double Master of Science degree from Université Jean Monnet, France, and the University of Eastern Finland, in 2010. He is currently pursuing the Ph.D. degree with the School of Electrical Engineering and Informatics, Institut Teknologi Bandung. He is currently a Lecturer with the Computer Engineering and Informatics

Department, Politeknik Negeri Bandung, Indonesia. He is the author of the book titled *Digital Image Processing: Theory and Real Applications* (Pengolahan Citra Digital: Teori dan Aplikasi Nyata). His research interests include digital image processing, computer vision, deep learning, and biomedical engineering.



TATI L. E. R. MENGKO received the bachelor's degree in electrical engineering from the Institut Teknologi Bandung, Bandung, Indonesia, in 1977, and the Ph.D. degree from the École Nationale Supérieure d'Électronique et de Radioélectricité de Grenoble (ENSERG), Institut National Polytechnique de Grenoble, France, in 1985, where she studied texture-based image processing. Since 2005, she has been a Professor with the School of Electrical Engineering and Informatics, ITB.

She is currently the Head of the Biomedical Engineering Research Group, ITB. Her research interests include biomedical signal and image processing. In 2015, she was granted the Innovation Award from ITB due to her contribution to developing a non-invasive vascular analyzer device. She has chaired numerous conferences, including the International Conference on Instrumentation, Communication, Information Technology, and Biomedical Engineering (ICICI-BME).



RINALDI MUNIR received the bachelor's degree in informatics engineering and the M.Sc. degree in digital image compression from the Institut Teknologi Bandung, Bandung, Indonesia, in 1992 and 1999, respectively, and the Ph.D. degree from the School of Electrical Engineering and Informatics, ITB, in 2010, where he studied image watermarking. In 1993, he started his academic career as a Lecturer with the Informatics Department, ITB. He is currently an Associate

Professor with the School of Electrical Engineering and Informatics, ITB, where he is also affiliated with the Informatics Research Group. His research interests include cryptography and steganography-related topics, digital image processing, fuzzy logic, and numerical computation.



ANGGRAINI BARLIAN received the bachelor's degree in biology from the Institut Teknologi Bandung, Bandung, Indonesia, in 1987, the master's degree from the University of Waterloo, Canada, in 1990, and the Ph.D. degree in biology from the Biology Department, ITB, in 1999. In 1988, she started her career as a Lecturer with the Biology Department, ITB. She is currently an Associate Professor in cell biology with the School of Life Sciences and Technology, ITB. Her

research interests include tissue engineering, developmental biology, reproductive biology, and aging.

...